Step Crowding Effects Dampen the Stochasticity of Crystal Growth Kinetics

James F. Lutsko,[1] Alexander E. S. Van Driessche,[2] Miguel A. Durán-Olivencia,[3] Dominique Maes,[2] and Mike Sleutel[2,*]

[1]*Center for Nonlinear Phenomena and Complex Systems, Code Postal 231, Université Libre de Bruxelles, Boulevard du Triomphe, 1050 Brussels, Belgium*

[2]*Structural Biology Brussels, Vrije Universiteit Brussel, Pleinlaan 2, 1050 Brussels, Belgium*

[3]*Complex Multiphase Systems, Department of Chemical Engineering, Imperial College, London, United Kingdom*

(Received 20 October 2015; published 6 January 2016)

Crystals grow by laying down new layers of material which can either correspond in size to the height of one unit cell (elementary steps) or multiple unit cells (macrosteps). Surprisingly, experiments have shown that macrosteps can grow under conditions of low supersaturation and high impurity density such that elementary step growth is completely arrested. We use atomistic simulations to show that this is due to two effects: the fact that the additional layers bias fluctuations in the position of the bottom layer towards growth and by a transition, as step height increases, from a 2D to a 3D nucleation mechanism.

DOI: 10.1103/PhysRevLett.116.015501

The dynamics of elementary steps determine to a large extent the kinetics of crystal growth from vapor and solution. The unperturbed motion of an isolated, elementary step as described in theory, is, however, rarely realized during the growth of any real crystal. Rather, steps tend to interact, and either repel or attract each other [1]. Consequently, the collective motion of a train of equidistant steps is in most cases inherently unstable and tends to decay into the grouping of those steps into bunches separated by areas relatively devoid of steps. In the limiting case where the interstep distance in a bunch becomes zero, a so-called true macrostep is formed [2]. The mutual attraction between steps arises from the competition for growth units and sets in when the diffusion field that supplies a step starts to overlap with the diffusion field of a neighboring step. Complicating factors are solutal flows perpendicular to the mean step orientation [3,4], asymmetric incorporation kinetics into upward and downward steps for the case of supply through surface diffusion [5–7], and the presence of impurities that dynamically adsorb and desorb from the terraces [8].

Kinematic descriptions of macrostep motion date back to the 1950s [9] and find their origin in theories developed to describe traffic flow and the onset of jamming [10]. Similar to cars, steps are predicted [11] to decelerate when in close proximity to one another. An exception to that prediction was published as late as 1999, with the discovery of the macrostep-mediated recovery of impurity poisoned surfaces for the potassium dihydrogen phosphate/Fe^{3+} system [12]. Counterintuitively, step bunches that populate the {100} KDP surface can advance under conditions where elementary steps are firmly fixed in place due to the action of terrace-bound stoppers. The authors developed a heuristic model that focused solely on the detachment of trailing steps from the macrostep's end, but ignored the question of why macrosteps start moving in the first place. In 2013, Ranganathan and Weeks [13] revisited the KDP/Fe system in simulation but focused on conditions outside of the dead zone for elementary steps. Their work elegantly shows how overlapping time scales of impurity adsorption and terrace exposure can lead to step bunching and ultimately to surface cleansing, but they do not address the fact that macrosteps can breach the impurity fence below the dead zone supersaturation. This simple observation is in direct contradiction with any theoretical models developed to date, and continues to challenge our understanding of crystal growth.

The occurrence of such a discrepancy between theory and experiment need not be surprising if one realizes that our current picture of crystal growth is based on incomplete physics. We recently showed that an explicit treatment of the terrace-step-kink model can expose unanticipated physics that are overlooked in mean-field approaches or during the development of analytical expressions [14,15]. The groundwork we performed using kinetic Monte Carlo simulations for elementary steps now allows us to investigate the dynamics of macrostep movement and its response to a field of impurities. Despite their relevance to crystal growth perfection, macrosteps remain elusive because they have so far resisted clear experimental characterization at the molecular level since even state-of-the-art *in situ* techniques are blind to their microscopic structure. In this Letter, we revisit the dynamics of macrosteps by means of atomistic simulation. Our work makes clear the mechanism that allows macrosteps to be mobile while elementary steps are pinned. This is of significant relevance to the fields of mineralogy, geochemistry, and biomineralization, that have long been faced with an apparent contradiction: most minerals in nature are grown from low supersaturation or low purity conditions, i.e., conditions that are traditionally linked with crystal growth cessation [16] due to impurity poisoning. Our work demonstrates that macrosteps, which are abundant surface

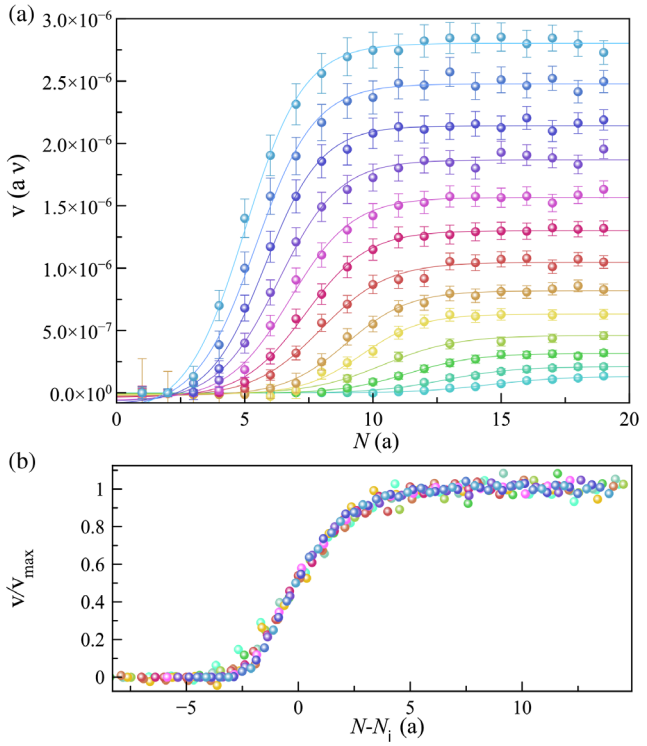

FIG. 1. (a) Velocity v as a function of macrostep height N (in units of atomic step size a) for a range of supersaturation values starting from 0.013ϵ (cyan) to 0.037ϵ (blue) at 0.002ϵ increments. Lines correspond to fits using $v = v_{\max} + (v_{\text{single}} - v_{\max})/\{1 + \exp([N - N_i)/\Delta N]\}$. ν is the kMC attempt frequency. (b) Master curve obtained by plotting the curves in (a) using reduced coordinates.

features on a wide range of crystals [17,18], provide an escape route from surface poisoning that explains how minerals can grow in such adverse growth environments.

For simplicity, we work on the (001) Kossel surface in the kinetically limited regime. Under these conditions, macrosteps are intrinsically unstable when no impurities are present on the surface. Indeed, we found that *ad hoc* generated macrosteps composed of N elementary steps rapidly decayed into step trains as a result of the entropic repulsion between the steps. However, when we populated the surface with a fixed density of impurity atoms, macrosteps relaxed into step bunches—with finite interstep distance—that were stable over the entire range of tested supersaturation. In a first instance we worked with regular impurity arrays with a fixed interimpurity distance in both directions.

We monitored the kinetics of growth for a broad range of step heights N and supersaturation values within the dead zone for elementary steps. A family of curves was obtained that exhibit sigmoidal dependencies of the mean macrostep velocity as a function of N which plateau to a supersaturation dependent value as shown in Fig. 1(a). These data convolute two physical effects: namely, the macrostep-mediated breaking of the impurity fence that is the focus of this work, and the Gibbs-Thomson effect as a result of step bending.

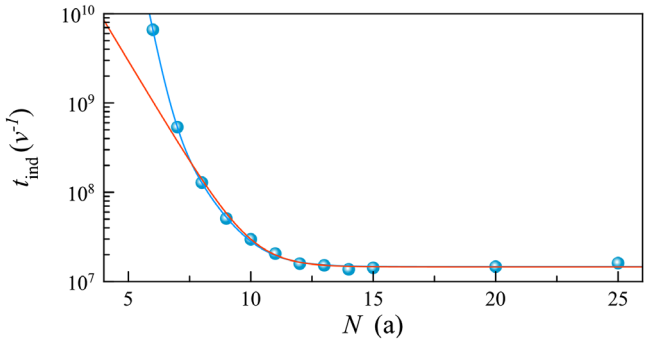

FIG. 2. The time t_{ind} required for a macrostep to break through a column of equidistant, surface bound impurities for $\Delta\mu = 0.017\epsilon$. The blue line corresponds to a fit using $t_{\text{ind}}(N) = A_1 \exp(-N/N_1) + A_2 \exp(-N/N_2) + A_3$, and the red line using $t_{\text{ind}}(N) = A_1 \exp(-N/N_1) + A_2$.

The supersaturation dependence of the latter can be accounted for by normalizing the measured macrostep velocities with their respective large-N values. We also note that the minimal step height required for growth recovery decreases as a function of supersaturation. If we correct the scaled velocities by shifting each individual curve with respect to its inflection point N_i, the master curve in Fig. 1(b) is obtained. This collapse suggests that the underlying mechanism which pushes macrosteps outside the kinetic dead zone is shared throughout the entire family of curves.

Inspection of the instantaneous macrostep velocity as a function of time reveals similar stop-and-go dynamics as has been reported for elementary steps near growth cessation [15]. The induction time associated with a macrostep fragment breaking through two neighboring impurity atoms exhibits a Poisson distribution (see Supplemental Material [19]), which is in accordance with the nucleation-limited kinetics expected for this regime of growth. Probing for the origin of the dependence of the growth rate on step height, we monitor the induction time t_{ind} as a function of N for a fixed supersaturation ($\Delta\mu = 0.017\epsilon$ with ϵ the bond energy; $N_i = 11.4 \pm 0.1$). The induction time decreases monotonically as a function of N, leveling out to a finite value for $N > 12$ (Fig. 2). It is clear that macrosteps of increasing height can move faster through a field of impurities by reducing the time spent in arrest in the stop-and-go regime. Three interesting features are worth stressing: (i) there is a minimum induction time associated with this nucleation process, i.e., there is a limit to how fast macrosteps can accelerate for a fixed surface impurity concentration, (ii) the value of N where $\min(t_{\text{ind}})$ is reached, does not correspond to the step height of maximum macrostep velocity ($N > 15$), and (iii) the experimental dependence in Fig. 2 follows a double exponential decay, rather than a single exponential decay as expected for classical nucleation. The last two points suggest that there is more than one mechanism by which t_{ind} can be reduced.

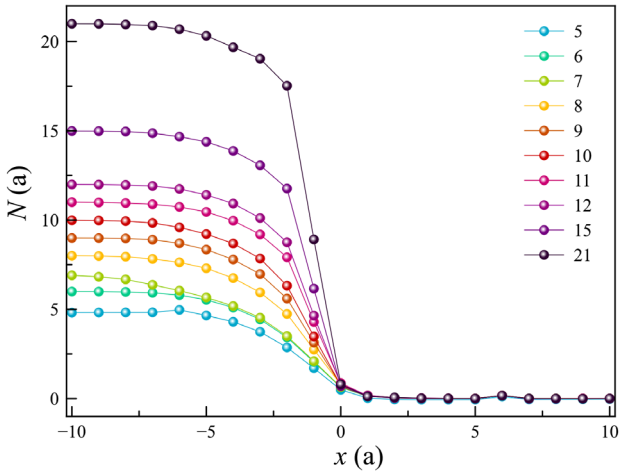

FIG. 3. Average macrostep structure as a function of step height N for $\Delta\mu = 0.017\epsilon$. x is the surface coordinate perpendicular to the mean step direction.

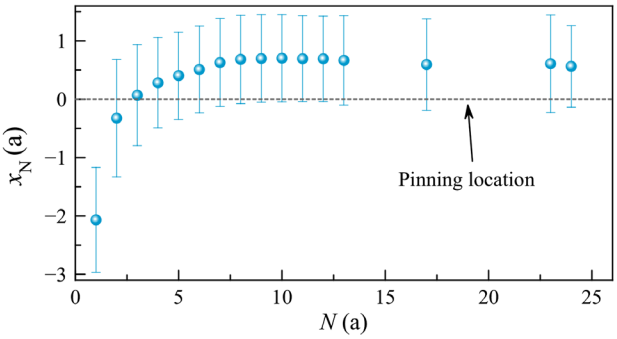

FIG. 4. Mean position $\bar{x}_N$ of the bottom step of a pinned macrostep as a function of N (with $N_i = 11.4 \pm 0.1$ for $\Delta\mu = 0.017\epsilon$).

To understand the origin of the observed t_{ind} dependence, we take a closer look at the macrostep structure as a function of N and $\Delta\mu$. More specifically, for a given (N, $\Delta\mu$) we calculate the spatial average of the macrostep topography followed by a temporal averaging during the period that the macrostep is pinned (Fig. 3). The step bunches exhibit a discontinuity in step density that becomes more pronounced for higher macrosteps and for higher supersaturation (see Supplemental Material [19]). The interesting feature is that the center of mass of the macrostep shifts closer to the pinning point as N or $\Delta\mu$ increases. The step bunches are essentially being compressed by the pressure exerted by the upper steps leading to ever decreasing interstep distances, which in the limit, leads to the formation of a facet with a simple crystallographic index (100). The steady-state pinned macrostep structure arises from a balance between the external, positive, supersaturated-induced pressure, and the internal negative pressure generated by the entropic repulsion. The gradual transformation towards a true macrostep has important consequences for the dynamics of the bottom, leading step that is being pinned by the impurities. This is of interest because the fluctuations of the bottom step are expected to determine to a large extent the rate of advancement of the entire macrostep [20].

As a measure of the dynamics of the bottom step, we monitored its mean position along the length of the step, x_N, as a function of time (see Supplemental Material [19]). As expected for a pinned single step, x_1 fluctuates randomly but is negative on average ($\bar{x}_1 < 0$); i.e., the center of mass is behind the pinning location. $\bar{x}_N$ increases monotonically as a function of N leveling out to a positive value for $N > 7$ (Fig. 4). This means that the fluctuations of the bottom step become gradually more biased towards positive fluctuations beyond the pinning location as the macrostep height increases. As negative fluctuations become gradually suppressed, the induction time to nucleate a supercritical fluctuation decreases, resulting in the measured increase in the macrostep growth rate. However, this dampening of the crystal growth stochasticity can only partially account for the v_{step} vs N dependence as it saturates much earlier, i.e., at $N \approx 8$ rather than $N = 15$. For that reason there must be an additional cooperative mode of step interaction that endows macrosteps to advance so quickly through an impurity field even when single steps are firmly pinned. A close inspection of the surface topography leading up to the moments of breakthrough reveals the nature of this secondary mechanism. Once a true macrostep is formed, local wetting of the intersection between the facet defined by the macrostep and the vicinal surface takes place. Dynamic three-dimensional clusters are formed which fluctuate, dissolve or grow (Fig. 5). Clusters that grow to supercritical sizes engulf the adjoining impurities and locally breach the impurity field, triggering the macrostep to *overflow* and advance until the next column of stoppers is encountered. As only macrosteps of increasing height gradually transform into true macrosteps (Fig. 3), it is clear to see why this 3D-nucleation mechanism only becomes active for larger values of N.

Now that we have established the mechanisms behind mutual step acceleration, we depart from the idealized scheme used so far, and move on to more realistic growth scenarios (see Supplemental Material [19]). First and foremost, we no longer limit the incorporation pathway of the primary growth units to direct impingement from solution, but allow surface diffusion as well. The general sigmoidal v_{step} dependence is recovered, with a slightly stronger dependence on N. Second, until now we have used neutral impurities that only interact with the terraces of the crystal; i.e., all interaction energies were set to zero apart from the downward interaction used to fix the impurities onto the surface. Both attractive as well as mildly repulsive solute-impurity interactions reproduce the general features of the master curve in Fig. 1. Third, rather than prepopulating the surface with a fixed density of impurities, we allow for continuous adsorption and desorption from the surface resulting in a random, dynamic distribution of impurities.

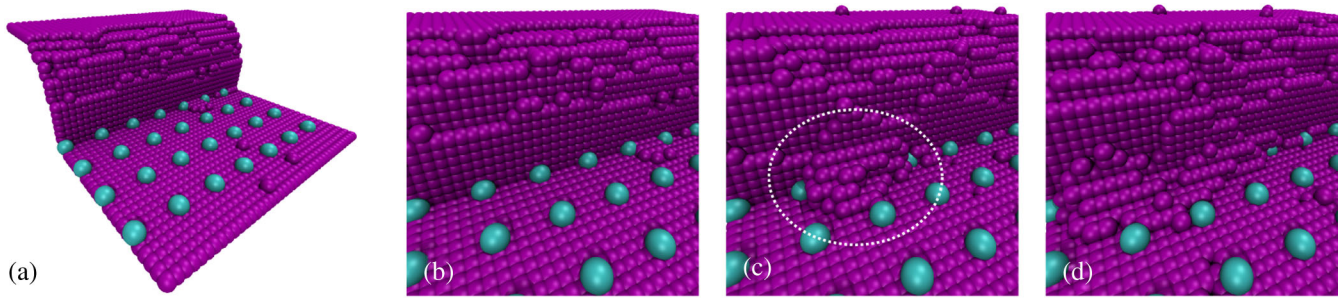

FIG. 5. Growth recovery mechanism for larger N values on true macrosteps: nucleation of a 3D cluster on the intersection between the vicinal surface and the facet defined by the macrostep.

We target conditions where the characteristic exposure times of impurity binding sites overlap with the inverse rate of impurity adsorption, leading to nonequilibrium surface concentrations as the macrosteps traverse the surface. Again, we recover the same result: elementary steps remain pinned, and macrosteps move at a rate that scales with their height. The interesting additional feature that is uncovered is that the uppermost, trailing step has the tendency to sporadically break free from the macrostep and becomes pinned in the process (see Supplemental Material [19], video). This is a key experimental observation for the KDP/Fe^{3+} system that is explained by the macrostep structure determined in this work: the interstep distance gradually increases towards the trailing end of the macrostep, which leads to an increased probability for impurity binding, leading to step pinning in the limit.

Our results emphasize the critical importance of fluctuations in the growth kinetics of crystals—fluctuations that are typically overlooked or averaged out in mean-field, mesoscopic, or analytic crystal growth treatments. The macrostep-mediated breaking of the impurity fence is a cooperative process driven by crowding of the constituent steps. The physics of step crowding can be captured using a simple random walk model. We imagine the steps to be abstracted as random walkers on a one-dimensional lattice that shifts to the right with probability p and to the left with probability $q = 1\text{-}p$. Nonzero supersaturation translates into asymmetric probabilities: $p > q$ giving rise to an average drift velocity $c = a(p - q)/\tau$, where a is the lattice spacing. A line of impurities can only be passed after the passing of a nucleation activation barrier. The simulations show that the first walker makes more crossing attempts if other walkers are present. In fact, a simple argument (see Supplemental Material [19]) indicates that the mean-first passage time for crossing the barrier will scale as $1/N$ where N is the height of the macrostep. We therefore expect the induction time for a macrostep to behave as $t_{\mathrm{ind}}(N) = t_0 + [t_{\mathrm{ind}}(1) - t_0]/N$, where t_0 is the minimum possible time to cross the barrier. In turn, the average velocity will be

$$v(N) = \frac{L}{t_{\mathrm{ind}}(N) + L/v_0} = \frac{v_0 L}{v_0 t_0 + L + v_0 t_{\mathrm{ind}}(1)/N}, \quad (1)$$

where v_0 is the macrostep velocity in the absence of impurities and L the distance between lines of impurities. This assumes that only the lowest elementary step is involved in the barrier crossing—all other steps pass unimpeded, as would be the case when breaking through the impurities occurs via 2D nucleation. When the case of 3D nucleation dominates, multiple steps n will be involved in the barrier crossing and the factor N in the velocity will be reduced to approximately $N - n$. This simple model reproduces the general trend in Fig. 1(b) and therefore gives some intuition as to how the *pressure* of the trailing steps increases the macrostep velocity in the presence of impurities and an idea as to the origin of the slow approach to a steady-state velocity with increasing step height.

Our results clearly show why macrosteps are able to move even when elementary steps are firmly pinned: (i) they stabilize the step structure required to pass a group of impurities and (ii) they facilitate the formation of a 3D nucleus that breaches the impurity fence. The bunching of steps effectively dampens the stochasticity of crystal growth by lowering the induction time, and by doing so, leads to a net acceleration. From the perspective of crowding, this is interesting because crowding is typically associated with subdiffusive behavior [21–23]. Macrostep-mediated recovery is a clear example of a molecular process that is accelerated rather than decelerated as a consequence of crowding.

The work of J. F. L., A. E. S. V. D, D. M., and M. S. is supported in part by the European Space Agency under Contract No. ESA AO-2004-070. The work of M. A. D-O. is supported by the European Research Council via Advanced Grant No. 247031.

*Corresponding author
msleutel@vub.ac.be

[1] R. Feigelson, *50 Years Progress in Crystal Growth: A Reprint Collection* (Elsevier, New York, 2004).
[2] A. A. Chernov, *Modern Crystallography III. Crystal Growth* (Springer-Verlag, Berlin, 1984).
[3] A. A. Chernov, J. Optoelectron. Adv. Mater. **5**, 575 (2003).
[4] S. R. Coriell, B. T. Murray, A. A. Chernov, and G. B. McFadden, J. Cryst. Growth **169**, 773 (1996).

[5] R. L. Schwoebel and E. J. Shipsey, J. Appl. Phys. **37**, 3682 (1966).
[6] R. L. Schwoebel, J. Appl. Phys. **40**, 614 (1969).
[7] O. Pierre-Louis, M. R. D'Orsogna, and T. L. Einstein, Phys. Rev. Lett. **82**, 3661 (1999).
[8] D. Kandel and J. D. Weeks, Phys. Rev. B **49**, 5554 (1994).
[9] W. K. Burton, N. Cabrera, and F. C. Frank, Phil. Trans. R. Soc. A **243**, 299 (1951).
[10] M. J. Lighthill and G. B. Whitham, Proc. R. Soc. A **229**, 317 (1955).
[11] A. A. Chernov, Sov. Phys. Usp. **4**, 116 (1961).
[12] T. A. Land, T. L. Martin, S. Potapenko, G. T. Palmore, and J. J. D. Yoreo, Nature (London) **399**, 442 (1999).
[13] M. Ranganathan and J. D. Weeks, Phys. Rev. Lett. **110**, 055503 (2013).
[14] J. F. Lutsko, N. González-Segredo, M. A. Durán-Olivencia, D. Maes, A. E. S. Van Driessche, and M. Sleutel, Cryst. Growth Des. **14**, 6129 (2014).
[15] M. Sleutel, J. F. Lutsko, D. Maes, and A. E. S. Van Driessche, Phys. Rev. Lett. **114**, 245501 (2015).
[16] S. Whitelam, Y. R. Dahal, and J. D. Schmit, arXiv: 1510.05619.
[17] I. Sunagawa, *Crystals: Growth, Morphology, & Perfection* (Cambridge University Press, Cambridge, England, 2005).
[18] B. Jamtveit and P. Meakin, *Growth, Dissolution and Pattern Formation in Geosystems* (Springer Science & Business Media, New York, 2013).
[19] See Supplemental Material at http://link.aps.org/supplemental/10.1103/PhysRevLett.116.015501 for details on seven supporting figures and a methods section.
[20] Note that in these simulations, with static impurities, only the bottom step interacts with the impurities.
[21] M. Weiss, M. Elsner, F. Kartberg, and T. Nilsson, Biophys. J. **87**, 3518 (2004).
[22] J.-H. Jeon, V. Tejedor, S. Burov, E. Barkai, C. Selhuber-Unkel, K. Berg-Sørensen, L. Oddershede, and R. Metzler, Phys. Rev. Lett. **106**, 048103 (2011).
[23] E. Barkai, Y. Garini, and R. Metzler, Phys. Today **65**, No. 8, 29 (2012).